

Structural, Electrical and Magnetic Properties of Cobalt Copper Ferrite Nanoparticles Prepared by sol–gel method.

Zena Mohammed Ali Abbas

*Department of physic, College of Science ,University of Diyala.,Iraq.
Email: zenaalbana@yahoo.com*

Abstract

In this paper nanoparticles of cobalt copper ferrite have been synthesized using sol–gel method were sintering at 1000°C for 2 hour. We report structural(Lattice Parameter , densities, Porosity, Volume), electrical and magnetic properties of $\text{Co}_{1-x}\text{Cu}_x\text{Fe}_2\text{O}_4$ (where $x=0.4$ and 0.8) ferrite nanoparticles. Analysis of structural properties has been carried out by using XRD and reveals that all samples have single phase cubic spinel structure. The XRD pattern showed that the synthesized nanoparticles were the crystalline in nature with average crystalline size of 34.84 and 34.97 nm by using Scherrer's formula. SEM micrograph were analysed to investigate the grain structure . M-H curves were calculated using magnetic hysteresis loop measurements. The permittivity (ϵ), dielectric loss ($\tan \delta$) were determined at room temperature as a function of frequency by using LCR meter. The frequency increases both real and imaginary parts of permittivity decrease exponentially.

Keywords: $\text{Co}_{1-x}\text{Cu}_x\text{Fe}_2\text{O}_4$, sol–gel method, magnetic properties, dielectric loss.

INTRODUCTION

The use of ultrafine magnetic media in the magnetic recording industry has long been recognized as a performance advantage. The different from those of the bulk materials due to their extremely small size and large specific surface area [1,2]. More precisely, some magnetic properties, such as saturation magnetization and coercivity, depend strongly on the particle size, morphology and microstructure of the materials. Scientists and engineers are nowadays interested in nanoscale which is from 1nm to 100nm. At nanoscale the properties of materials are very different from those at a larger scale. Therefore, the nano-world is in between quantum world and macro world. Nanoscience is concerned with the study of phenomena and manipulation of materials at nanometer scales. Nanotechnology is the design, characterization, production and application of structures, devices and system controlling shape and size at the nanometer scale. The electromagnetic properties of nanoferrites are very sensitive to many factors, including the method of preparation, sintering rate, sintering temperature, sintering duration and sintered additives [3]. The material science research is focused on the invention of new materials with the enhanced properties and novel synthesis techniques to cope up with the increased technological demand. Nanocrystalline materials are the centre of the attention due to their tremendous applications and interesting properties. The properties of nanomaterials are remarkably different than that

of their bulk counterpart. The interest in the ferrite nanoparticles is due to their important physical and chemical properties for various technological applications such as high density magnetic storage, bubble devices, electronic communication devices, sensors, magnetically guided drug delivery [4–5]. Various methods have been developed for the synthesis of nanoferrites, like sonochemical reactions, sol-gel, microwave plasma, host template, coprecipitation, microemulsion and chemical vapour deposition [6]. The sol–gel process (including a heat treatment operation) is probably the most effective and feasible route to develop high purity, homogeneous and crystalline nanoparticles. The sol–gel technique is a low temperature process which involves hydrolysis and condensation reactions of metal precursors (salts or alkoxides) leading to the formation of a three-dimensional inorganic network [7,8], electrical and magnetic properties of ferrites depend upon the nature of the ions, their charges and their distribution among tetrahedral (A) and octahedral (B) sites [9], the present work reports the structural, and magnetic properties of copper substituted cobalt ferrites having the general formula $\text{Co}_{1-x}\text{Cu}_x\text{Fe}_2\text{O}_4$; $x = 0.4, 0.8$ prepared using citrate precursor method.

Experimental

The sol–gel synthesis was based on the formation of a stable and homogenous solution made by dissolving a mixture of cobalt nitrate $\text{Co}(\text{NO}_3)_2 \cdot 6\text{H}_2\text{O}$, Copper nitrate $\text{Cu}(\text{NO}_3)_2$, ferric nitrate $\text{Fe}(\text{NO}_3)_3 \cdot 9\text{H}_2\text{O}$. In this method each sample was prepared by taking the desired proportion of analytical reagent grade precursor nitrates, which were separately dissolved in 20 ml of double distilled water. Molar ratios between metal nitrates and the reducing agent were calculated by oxidized and reduced valence states of various elements. All the solutions were mixed together and citric acid was added as fuel for auto combustion. The solutions were evaporated with continuous stirring till gel formation on a hot plate (Heat and Stir, Glassco, India) and the hot plate temperature was set at 200°C in an oven until they turned into brown color fluffy mass. Thus the formed gel ignites itself, resulting into nanoparticles of desired ferrite. These obtained ferrites were then heat treated to 1000°C for 2 h. For electric measurements the samples were pressed into circular disc shaped pellets and silver pasting was applied on the opposite faces to make parallel plate capacitor geometry with ferrite material as the dielectric medium. Nanoparticles of copper substituted cobalt ferrites $\text{Co}_{1-x}\text{Cu}_x\text{Fe}_2\text{O}_4$ (where $x=0.4$ and 0.8) were prepared using sol–gel method compounds were checked by X-ray diffraction (XRD) patterns. The XRD patterns of all the samples at room-temperature were obtained

using a X-ray diffractometer (Rikagu Miniflex, Japan) with CuK α radiation $\lambda = 1.5405\text{\AA}$ between the Bragg angles 10° to 100° .

RESULTS AND DISCUSSION

Structural properties

XRD analysis

Fig.1 shows the room temperature XRD profiles of $\text{Co}_{1-x}\text{Cu}_x\text{Fe}_2\text{O}_4$ (where $x=0.4$ and 0.8) compounds sintering at 1000°C obtained from sol-gel methods. The XRD patterns showed the presence of little broadened peaks. The broad peaks indicate particles having smaller crystallite size. The peaks at 30.46 , 35.84 , 43.46 , 54.5 , 57.32 , and 62.92 are indexed as the reflection planes of (220), (311), (400), (422), (511), and (440), respectively. Analysis of the XRD patterns of all samples confirmed the formation of the cubic spinel structure as the main characteristic peak. The reflection plane (311) was used to calculate both the crystallite size and lattice constant since this has the maximum diffraction intensity. All the peaks of the XRD pattern are indexed by JCPDS as reported on ASTM cards (cards 1-1121 and 3-0864). The values obtained from the analysis of XRD data lie within the expected range of the lattice constant of spinel cubic ferrites [10]. The calculated lattice constant a (using the d value and respective hkl (311) parameters) was calculated according to the formula:

$$a = d_{hkl} \sqrt{h^2 + k^2 + l^2} \dots\dots\dots(1)$$

The apparent particle sizes of all the compounds were estimated by analyzing the X-ray diffraction peak broadening, using Scherrer's formula[11]:

$$D = 0.9\lambda / \beta \cos \theta \dots\dots\dots(2)$$

where λ is the wavelength of the radiation, θ is the diffraction angle, and β is the full width at half maximum (FWHM), data yielded the cubic unit cell structure for $\text{Co}_{1-x}\text{Cu}_x\text{Fe}_2\text{O}_4$. The lattice parameters as obtained are depicted in Table 1:

The X-ray density (theoretical) is calculated by using the following relation:

$$D_{hkl} = \frac{8M}{N a^3} \dots\dots\dots(3)$$

where M is the molecular weight of the compound of ferrite sample, 8 represents the number of molecules per unit cell, N the Avogadro's number, and ' a ' lattice constant. The apparent density (experimental) of the circular shape pellet is calculated by using the following relation:

$$D = \frac{m}{v} = \frac{m}{\pi r^2 h} \dots\dots\dots(4)$$

where m , V , r and h represent the mass, volume, radius and the thickness of the pellet, respectively. The X-ray density depends on the lattice constant and the molecular weight of the sample, while the theoretical density of the samples is calculated from the geometry and mass of the samples. It can be seen from Table 1. The higher value of X-ray density than that of the apparent density is due to the existence of pores that depend on the sintering conditions [12].

and the calculation of porosity using the formula [13]:

$$\text{Porosity} = [(1-D)/D_{hkl}] * 100\% \dots\dots\dots(5)$$

The porosity of the samples as shown in Table 1, increases with Cu^{2+} substitution; this is due to the lower density of doping ions.

Table 1. Lattice parameters derived from X-ray diffraction pattern of $\text{Co}_{1-x}\text{Cu}_x\text{Fe}_2\text{O}_4$ ferrites sintered at 1000°C for 2h.

x	Molar Ferrite Composition	Lattice Parameter, a (\AA)	Densities (g/cm^3)		Crystallite size (nm)	Porosity (%)	Volume(a^3)
			Dtho	Dexp			
0.4	$\text{Co}_{0.6}\text{Cu}_{0.4}\text{Fe}_2\text{O}_4$	8.413	4.593	2.94	34.84	36	595.46
0.8	$\text{Co}_{0.2}\text{Cu}_{0.8}\text{Fe}_2\text{O}_4$	8.432	4.563	2.76	34.97	40	599.50

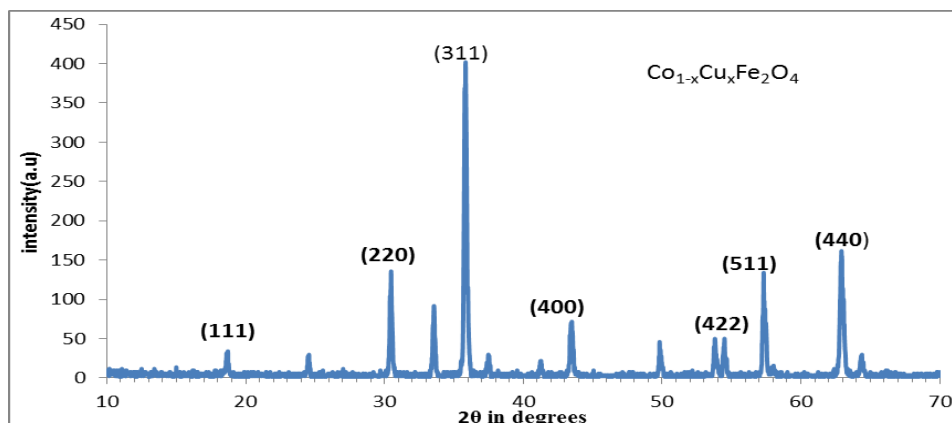


Figure.1. XRD pattern synthesis of $\text{Co}_{1-x}\text{Cu}_x\text{Fe}_2\text{O}_4$ ferrite sintered at 1000°C .

Scanning electron microscopy (SEM)

Fig.2 shows the SEM images of the synthesized $\text{Co}_{1-x}\text{Cu}_x\text{Fe}_2\text{O}_4$ ferrite nanopowders. SEM micrograph was analysed to investigate the grain structure of the nanopowder and assist in understanding the development of the grain sizes. Fine grain growth is found in the sample by a closer look at these microstructures, it is found that the grains in the sample are spherical in shape [14]. particles with irregular shapes and some agglomeration where particles form large clusters. This

image has been used to estimate the particle size distribution. The sample is composed of nanoparticles in the size range about 34 nm. The asymmetric shape of the histogram may indicate that some agglomeration had taken place, with the formation of particles with larger sizes. The rate of grain growth and the resultant microstructure depend in a complex way on many factors, such as the sintering temperature, the oxygen partial pressure, stoichiometry

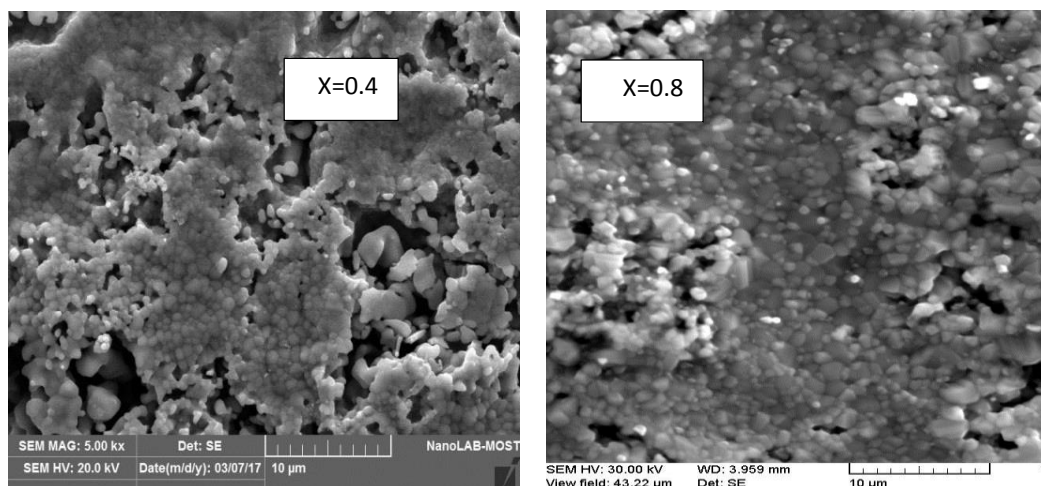


Figure.2. Scanning electron micrographs of $\text{Co}_{1-x}\text{Cu}_x\text{Fe}_2\text{O}_4$ ($x=0.4,0.8$) ferrite nanoparticles

In a cubic system like ferromagnetic spinels, the magnetic order is mainly because of the mechanism of super exchange interaction taking place in between metal ions in A and B sub lattices. The substitution of paramagnetic ions such as divalent copper having preferential A site occupancy results in an increase in the exchange interaction between A and B sites [15]. Hence, on changing the concentration of copper in cobalt copper ferrites, it would be possible to vary their magnetic Properties.

Magnetic measurement

Fig. 3 shows the hysteresis loop for $\text{Co}_{1-x}\text{Cu}_x\text{Fe}_2\text{O}_4$ ferrite. It shows the magnetization versus applied field (M-H) curve of the synthesized samples obtained by using a vibrating sample magnetometer (VSM) at room temperature. Different magnetic parameters such as magnetization (M_s), and coercivity (H_c) were estimated from M-H curves were calculated using magnetic hysteresis loop measurements. It is observed that the saturation magnetization decreases with increasing the copper ion concentration. In the ideal situation, when the prepared

sample grows into a pure inverse type spinel structure with all Co^{2+} ions located in the octahedral sub-lattice. It can be seen that mixing of cobalt with copper ferrite changes the coercivity and magnetization values and show a very small coercive field. This could be due to the fact that less number of magnetic ion $\text{Co}^{2+}\text{-Fe}^{3+}$ pairs is formed, as Cu^{2+} ion is diamagnetic in nature, which is responsible for marked decrease the value of magnetization. This might result in giving small coercive field and retentivity [16], in this case it should be noted that no heat treatment was carried out at the end of the synthesis process. This omission could have had the effect that the particles might have been only partially crystalline and, in turn, this factor may have contributed to a reduction of the effective size of the particles. Particle size has an important role in decreasing the saturation magnetization and therefore the omission of the heat treatment casts some doubt on the very low value for the saturation magnetization quoted in this reference. The low result for saturation magnetization might be as well due to the presence of organic materials in the sample. It is now necessary to investigate the magnetic properties at low temperature.

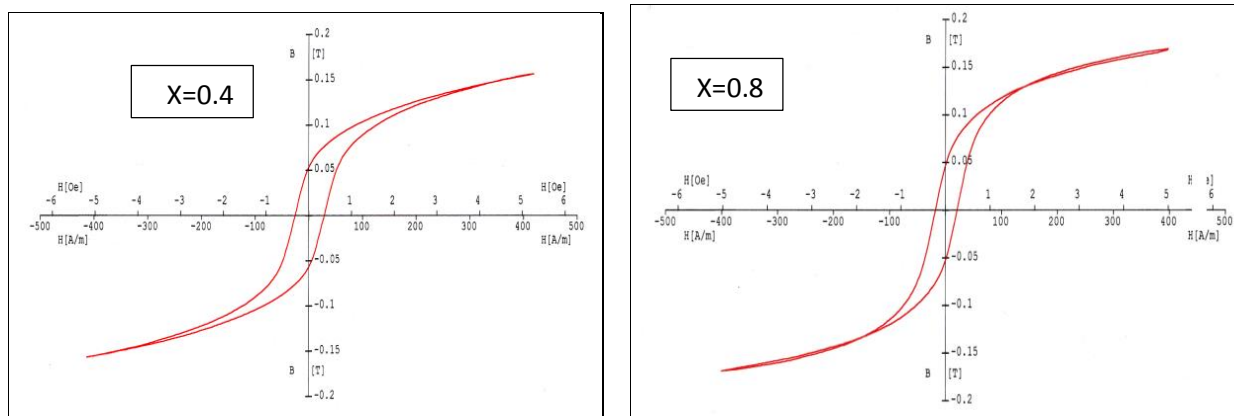


Figure.3. Hysteresis loop of $\text{Co}_{1-x}\text{Cu}_x\text{Fe}_2\text{O}_4$ ferrite (for $x = 0.4, 0.8$) nanoparticles samples sintering at 1000°C .

Electrical properties.

The dielectric and impedance spectroscopy measurements, as a function of frequency at room temperature, were performed by using LCR meter is Agilent impedance analyzer an American origin, its range of frequency is (50Hz-5MHz). The permittivity (ϵ') of the samples has been calculated using the formula:

$$\epsilon' = \frac{C_p \times d}{\epsilon_0 \times A}$$

where C_p is the capacitance of the parallel plate capacitor in F, d is the thickness in cm and A is the cross-sectional area in cm^2 of the pellet and ϵ_0 is the free space permittivity. The complex permittivity has been determined using the following relation:

$$\epsilon'' = \epsilon' \tan \delta$$

where $\tan \delta$ is the dielectric loss factor which gives the loss of energy from the applied field into the sample (energy dissipated in the form of heat). The loss tangent ($\tan \delta$) of the materials is related to the resistivity of the sample by this relation:

$$\tan \delta = \frac{1}{2\pi f \epsilon_0 \epsilon' \rho}$$

Here f is the frequency of the applied field and ρ is the resistivity.

Figs. 4 represent the variation of the dielectric loss with frequency at room temperature for $\text{Co}_{1-x}\text{Cu}_x\text{Fe}_2\text{O}_4$ ferrite nanoparticles. It can be seen from Figs. 4 that as frequency increases the dielectric loss decrease exponentially. The decrease the dielectric loss is rather sharp in low frequency region, as frequency increases it remains almost constant for all the compositions under investigation. The decrease in the dielectric loss with frequency indicates that mechanism of polarization process in ferrites is similar to that of conducting process. The decrease of the polarization with increasing frequency may be due to the fact that beyond a certain frequency of the electric field the electronic exchange between ferrous and ferric ions cannot follow the alternating field.

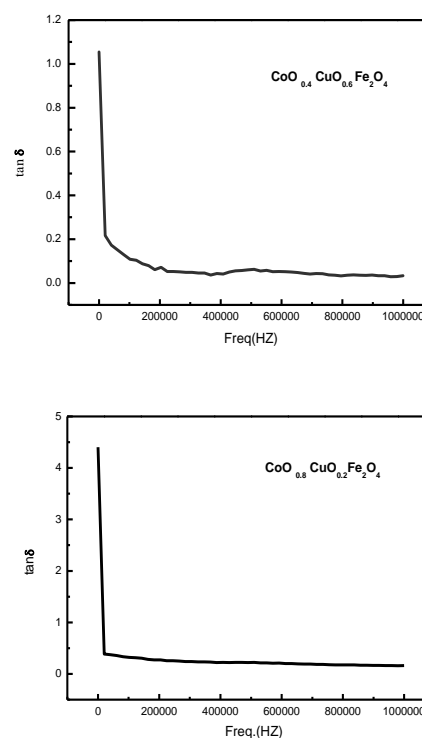


Figure. 4. Variation of dielectric loss ($\tan \delta$) as a function of freq. (Hz) of $\text{Co}_{1-x}\text{Cu}_x\text{Fe}_2\text{O}_4$

CONCLUSIONS

X-ray diffraction patterns confirm the formation of cubic spinel phase without any additional impurity peaks indicating successful synthesis of $\text{Co}_{1-x}\text{Cu}_x\text{Fe}_2\text{O}_4$ ($x=0.4$ and 0.8) compounds sintering at 1000°C by sol-gel process. The average crystallite size calculated from XRD data was found in 34.84 and 34.97 nm. The dielectric dispersion with frequency is explained on the basis of electron-hole hopping mechanism. All the samples show appreciable hysteresis with good value of saturation magnetization at room temperature.

REFERENCES

- [1] A. Animesh, C. Upadhyay and H.C. Verma, *Physics Letters A*, 311(2003)410.
- [2] D-H. Chen and Y-Y. Chen, *Journal of Colloid and Interface Science*, 235(2001)9. Remarkable
- [3] Xiang J, Shen X Q, Song F Z and Liu M Q 2009 *Chin.Phys. B* 18 4960
- [4] A. Goldman, *Modern Ferrite Technology*, 2nd ed., Springer, New York, 2006.
- [5] S.F. Mansour, M.A. Elkestawy, *Ceram. Int.* 37 (2010) 1175.
- [6] Kohli S, McCurdy P R, Johnson D C, Das J and Fisher E R 2010 *J. Phys. Chem. C* 114 19557
- [7] C.J. Brinker, G.W. Scherer, *Sol-Gel Science: The Physics and Chemistry of Sol-Gel Processing*, Academic Press, San Diego, 1990.
- [8] R. Corriu, N.T. Anh, *Molecular Chemistry of Sol-Gel Derived Nanomaterials*, John Wiley & Sons, UK, 2009
- [9] Baykal AI, Kasapoglu N, Koseoglu Yk, Toprak MS, Bayrakdar H: CTAB-assisted hydrothermal synthesis of NiFe₂O₄ and its magnetic characterization. *J Alloys Compd* 2008, 464(1-2):514-518.
- [10] A.A. Satar, H.M. El-Sayed, K.M. El-Shokrofy, M.M. El-Tabey, *J. Appl. Sci.* 5 (2005) 162.
- [11] B.D. Cullity, S.R. Stock, "Elements of X-Ray Diffraction" 3rd ed., Prentice Hall, New York,(2001).
- [12] M.A. Gabal, S.S. Ata-Allah, *Mater. Chem. Phys.* 85 (2004) 104.
- [13] MA Ahmed, NOKasha and S I El-Dek1" Preparation and characterization of nanometric Mn ferrite via different methods" *Nanotechnology* 19,(2008).
- [14] Y.-P. Fu, C.-H. Lin, C.-W. Liu, *J. Magn. Magn. Mater.* 283 (2004) 59.
- [15] Christensen AN, Lebech B, Andersen NH, Grivel J-C (2014) The crystal structure of paramagnetic copper(ii) oxalate (CuC₂O₄): formation and thermal decomposition of randomly stacked anisotropic nano-sized crystallites. *Dalton Trans* 43: 16754-16768.
- [16] R. K. Singh, A. Yadav, K. Prasad, A. Narayan, *Int. J. Engg. Sci. Technol.* 2 73 (2010).